

BNL-73190-2004-CP  
CAP-392-Accel-04C

**ELECTRON MODEL OF AN FFAG MUON ACCELERATOR**

*E. Keil*  
*CERN*

*J. Scott Berg*  
*Brookhaven National Laboratory*

*A. M. Sessler*  
*Lawrence Berkeley National Laboratory*

July 2004

# ELECTRON MODEL OF AN FFAG MUON ACCELERATOR

E. Keil\*, CERN, CH1211 Geneva 23, Switzerland, J.S. Berg†, BNL, Upton, Long Island, NY 11973-5000, USA, A.M. Sessler‡, LBNL, Berkeley, CA 94720, USA

## Abstract

Parameters are derived for the lattice and RF system of an electron model of a non-scaling FFAG ring for accelerating muons. The model accelerates electrons from about 10 to about 20 MeV, and has about 15 m circumference. Magnet types and dimensions, spacing, half apertures, about 12 mm by 20 mm, and number of cells are presented. The tune variation with momentum covers several integers, similar to that in a full machine, and allows the study of resonance crossing. The consequences of misaligned magnets are studied by simulation. The variation of orbit length with momentum is less than 36 mm, and allows the study of acceleration outside a bucket. A 100 mm straight section, in each of the cells, is adequately long for an RF cavity operating at 3 GHz. Hamiltonian dynamics in longitudinal phase space close to transition is used to calculate the accelerating voltage needed. Acceleration is studied by simulation. Practical RF system design issues, e.g. RF power, and beam loading are estimated.

## INTRODUCTION

Recently, there has been a revival of interest in the use of fixed field alternating gradient accelerators (FFAGs) for many applications, including muon accelerators, high-intensity proton sources, and possibly medical applications. The original FFAGs, and those recently built in Japan, have been based on a so-called scaling FFAG design, for which tunes are constant and the behaviour in phase space is independent of energy with the exception of a scaling factor. Recent interest has mostly focused on non-scaling designs, which while having the large energy acceptance that characterizes an FFAG, do not obey the scaling relations of the scaling FFAG. These designs have more modest magnets than scaling FFAGs, but involve transverse resonance crossing and novel acceleration methods.

Table 1: Lattice Parameters at 15 MeV Reference Energy

Number of cells	45	
Cell length	0.34	m
F/D magnet length	100/50	mm
F/D magnet angle	-54.333/193.959	mrad
F/D magnet gradient	5.030/-4.313	T/m
F/D magnet field	-27.170/96.699	mT

\* Eberhard.Keil@t-online.de

† jsberg@bnl.gov, supported by US Department of Energy contract DE-AC02-98CH10886

‡ AMSessler@lbl.gov, supported by the U.S. Department of Energy under Contract No. DE-AC03-76SF00098

Since no non-scaling FFAG has ever been built, there is interest in building a small model which would accelerate electrons and demonstrate our understanding of non-scaling FFAG design. In particular, the model should allow study of resonance crossing and rapid acceleration outside of RF buckets. We show how this goal can be attained.

## LATTICE

Tab. 1 shows the main parameters of the doublet lattice. For the coils and an RF cavity, 40 mm and 100 mm spaces are provided between the magnets. The focusing and defocusing gradient magnets are rectangular. Fig. 1 shows the optical functions  $\sqrt{\beta_x}$ ,  $\sqrt{\beta_y}$ , and dispersion  $D_x$ .

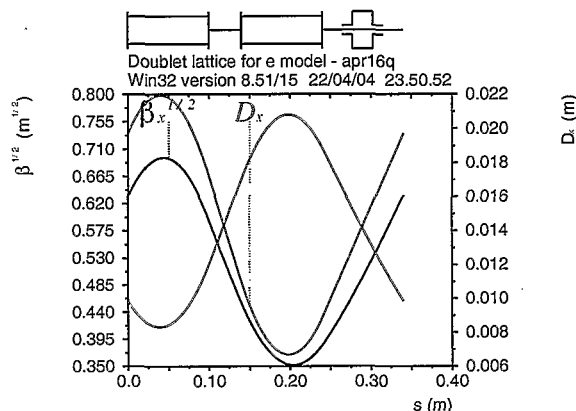


Figure 1: Orbit functions in a 0.34 m long doublet cell

The gradients are adjusted such that the phases advance by  $q_x = 0.233$  and  $q_y = 0.184$  in a cell at  $\delta p/p = 0$ , and remain well below the intrinsic half-integral stop band at  $q = 1/2$  at  $\delta p/p = -0.35$ . We use  $q$  for the tune of single cells, and  $Q$  for that in the whole ring. The bending angles are adjusted such that the flight time through a cell is nearly independent of the relative momentum error to first order near  $\delta p/p = 0$ . Fig. 2 shows the variation of the flight times with  $\delta p/p$  for a single lattice cell, from two calculations. The TWISS command in MAD [1] provides  $\delta(s)$ , the difference in path length between an off-momentum orbit and the reference orbit. The TRACK command, starting on the off-momentum closed orbit, yields  $ct$ , the difference in flight time between the off-momentum and the reference particle, multiplied by the speed of light  $c$ . The differences between  $\delta(s)$  and  $ct$ , although small, indicate that the MAD [1] calculation is not highly accurate. The slope of  $ct$  at  $\delta p/p = 0$  is zero by design, while that of  $\delta(s)$  is almost zero. The leading variation of  $\delta(s)$  and  $ct$  with  $\delta p/p$

is quadratic. The spread in flight times is less than about 30 mm for  $-0.33 \leq \delta p/p \leq 0.33$ . Fitting a parabola to  $ct$  near  $\delta p/p = 0$  yields the slip factor  $\eta_1$  listed in Tab. 3.

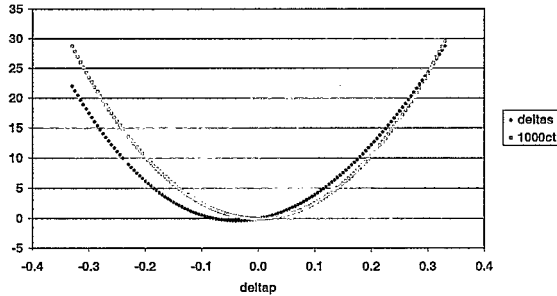


Figure 2: Variation of orbit length  $\delta s$  and flight time  $ct$  in mm for the ring with the relative momentum error  $\delta p/p$ .

## MAGNETS

The electron beam has a normalised RMS emittance  $\varepsilon_n = 0.3$  mm, between the values of the ATF [2] and the injector for CTF3 [3], such that the divergences in the model are close to those in a typical muon accelerator. Three RMS beam radii are allowed for in the half aperture  $A$ . In the horizontal plane, the betatron beam size is added to the orbit offset  $|x_c|$ . Hence,  $A_y \approx 8.5$  mm and  $A_x \approx 15.3$  mm are needed, for a momentum range  $-0.33 \leq \delta p/p \leq +0.33$ . This method of combining  $|x_c|$ ,  $\beta_x^{\max}$ , and  $\beta_y^{\max}$  surely overestimates  $A_y$  of the F magnets and  $A_x$  of the D magnets, and the pole tip field in the D magnets.

Tab. 2 shows the field and aperture parameters. The ratio of magnetic field and gradient  $B/G$  is the lateral distance between the reference orbit and the radius where the magnetic field vanishes. Allowing a few mm for closed orbit distortions yields the horizontal and vertical aperture radii  $A_x$  and  $A_y$ , respectively. In the F magnets,  $B/G$  is smaller than  $A_x$ ; hence, we propose displaced quadrupoles, rather than C or H shaped gradient dipoles. In the D magnets,  $B/G \approx 22.6$  mm is larger than  $A_x$ ; hence, we propose half quadrupoles with a neutral pole. With respect to the centre of the quadrupole, where  $B = 0$ , the horizontal aperture is in the ranges of  $x$  shown in Tab. 2. Assuming that the hyperbolic pole face passes through the point with the largest value of  $x$  and  $y = A_y$ , yields the bore radius  $r$ . The pole tip field  $B(r)$  follows from the gradients in Tab. 1. These pole tip fields are close to that achieved in the permanent-magnet quadrupoles of the Recycler at Fermilab [4].

## ACCELERATION

We propose to operate the model with the reference energy equal to the transition energy, and the lowest order slip factor  $\eta_0 = 0$ . Keeping only the slip factor  $\eta_1$  in the longitudinal Hamiltonian [5] in the variables phase,  $\varphi$ , measured in cycles, and momentum error,  $p_t$ , relative to the reference

Table 2: Field and Aperture Parameters

Magnet	F	D	
$B/G$	5.4	22.4	mm
$A_x/A_y$	$\pm 18/\pm 11$	$\pm 18/\pm 11$	mm
$x$	$-12.6 \dots 23.4$	$4.4 \dots 40.4$	mm
$r$	18.3	29.6	mm
$B(r)$	0.10	0.14	T

momentum  $p_r$ , and assuming stationary buckets, yields:

$$H_1(p_t, \varphi) = 2\pi\beta_r^2 E_r h \eta_1 p_t^3 / 3eV N_c + \sin^2 \pi\varphi. \quad (1)$$

Here,  $h$  is the harmonic number,  $V$  is the accelerating RF voltage in one of  $N_c$  cavities,  $\varphi$  is the phase angle, counted from the stable phase angle, and  $\beta_r$  and  $E_r$  are the speed in units of the light velocity, and energy of the reference particle. The first term in (1) may be taken as the cube of a scaled momentum variable  $y$ . In terms of  $y$  and  $\varphi$ , the Hamiltonian is  $H_2(y, \varphi) = y^3 + \sin^2 \pi\varphi$ . Particles are accelerated from  $y = -1$  at  $\varphi = 0.5$  to  $y = +1$  at  $\varphi = 0$ . The acceleration range in terms of  $p_t$  is:

$$p_t = (3eV N_c / 2\pi\beta_r^2 E_r h \eta_1)^{1/3}. \quad (2)$$

$N_c V$  is proportional to the cube of  $p_t$ ,  $h$  or  $f_{RF}$ , and  $\eta_1$  or the spread in flight times shown in Fig. 2. Exploring acceleration and resonance crossing over about an order of magnitude in the number of turns  $n$  is possible by simultaneously reducing  $p_t$  and  $N_c V$  according to (2). Much larger ranges of  $n$  can be studied with a second RF system operating at a lower frequency  $f_{RF}$ .

Table 3: RF System Parameters

Slip factor $\eta_1$	0.0167	
Number of cavities $N_c$	45	
RF frequency $f_{RF}$	3	GHz
RF cavity voltage $V$	66	kV
RF cavity power $P$	1015	W
Stored energy $W_s$	0.955	mJ
Range $p_t$ from (2)	$\pm 0.335$	
Initial/final $p_t$	$-0.330/+0.330$	
Number of turns $n$	4	
Beam current $I_b$	$\ll 71$	mA

Tab. 3 shows the parameters of the RF system. The accelerating ranges, calculated from (2), and found by tracking, adjusting the initial value of  $p_t$  such that the initial and final values of  $p_t$  have the same magnitude and opposite sign, agree well. The circumferential accelerating voltage,  $45 \times 66\text{kV} = 3$  MV, is a substantial fraction of the energy range, 10 MeV. Hence, the changes of  $p_t$  from turn to turn are substantial, as shown in Fig. 3, and only four turns are enough to reach the final  $p_t$ .

For a **longitudinal simulation in a perfect model** we launch nine particles at  $ct = 50 \pm 5$  mm with  $p_t = -0.328 \pm 0.03$ , and track them for five turns. They are

accelerated, and reach their maximum  $p_t$  after four turns at  $ct \approx 0$  mm, above the neighbouring stable fixed point. The normalised longitudinal phase space area enclosed by the particles is about 18 mm or about  $3 \times 10^{-5}$  eVs, larger than that achieved in ATF and CTF3 by at least a factor of 30. Particles launched at the central momentum error move more quickly than those at the higher and lower momentum errors, and cause a distortion of longitudinal phase space. Berg and Palmer have shown that this distortion can be removed by an RF system at the third harmonic [7].

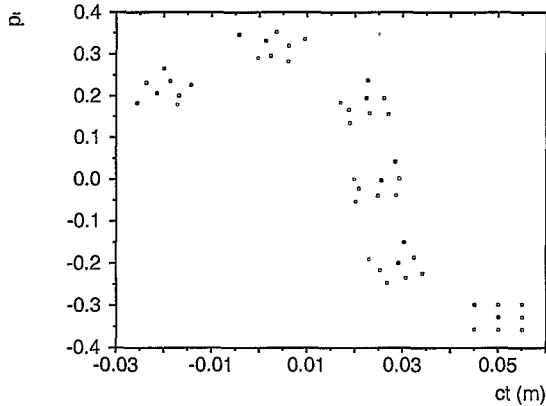


Figure 3: Acceleration in longitudinal phase space ( $ct, p_t$ ) in the perfect model with 2.97 MV peak circumferential RF voltage.  $V = 0$  at  $ct = 50$  mm and 0 m;  $V$  has the maximum at  $ct = 25$  mm, and the minimum at  $ct = -25$  mm.

For the **longitudinal simulation with transverse misalignments** we assume that the doublets are installed on girders with much better precision than 0.03 mm, the standard deviation of the girder alignment. The distribution of the displacements is a Gaussian, truncated at 2.5 standard deviations. Comparing Fig. 4 to Fig. 3 without misalignments shows very similar behaviour, and suggests that the imperfection resonances can be crossed.

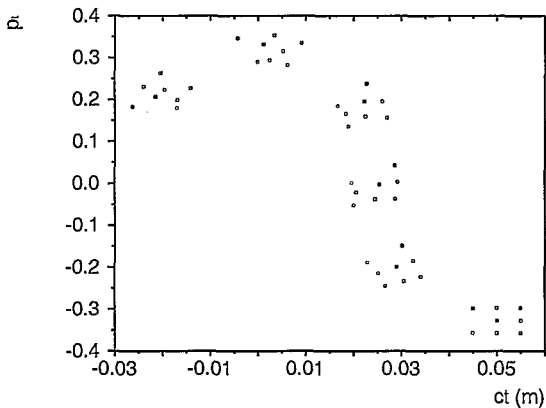


Figure 4: Acceleration in longitudinal phase space ( $ct, p_t$ ) in the model with 2.97 MV peak circumferential RF voltage. The magnets are installed on girders which are transversely displaced with 0.03 mm standard deviation.

## RF SYSTEM

Pillbox shaped RF cavities of copper with conductivity  $\sigma = 5.8 \cdot 10^7 / \Omega / \text{m}$  are installed in all 45 lattice cells, have intrinsic impedance  $R/Q = 121 \Omega$  and quality factor  $Q = 17733$  [6], neglecting the beam ports, and are very similar to typical buncher cavities in S band linacs. The RF power  $P$  in an RF cavity is  $P = V^2 / 2Q(R/Q)$ . Whether to install 45 RF cavities in all cells, or only every so often, is related to the optimisation of the RF system and the space needed for other equipment, e.g. injection and ejection kickers. Imposing the condition that the energy extracted by the beam from the RF cavities  $W_e = ICVn/c\beta_r$  is much smaller than the energy stored there  $W_s = V^2 / 4\pi f_{RF}(R/Q)$  yields an upper bound for the beam current  $I_b \ll V / [4\pi n h (R/Q)]$  in Tab. 3. This upper bound is pessimistic, since RF cavities in all cells are assumed. With fewer RF cavities,  $I_b$  would be higher. A calculation of transient beam loading, taking into account the variation of phase and acceleration shown in Fig. 3 is beyond the scope of this note. The beam observation system must work accurately enough at beam currents  $\ll I_b$ .

## CONCLUSIONS

We investigated a small electron model of a full scale Muon Non-Scaling FFAG Accelerator (from 10 to 20 GeV). We found that a device operating between 10 and 20 MeV, and with a circumference of only 15.3 m, and magnetic fields of less than 0.1 T, can model the novel features of a non-scaling FFAG; namely the crossing of transverse resonances and rapid acceleration outside of RF phase space buckets. Practical matters were considered and shown to all be within the present state of the art. More details can be found in [8]. In the near future, we envisage more complete simulations, we will address engineering issues, and search for parameters in wider ranges of energy, circumference, slip factors  $\eta_0 \neq 0$  and  $\eta_1$ .

## REFERENCES

- [1] H. Grote, F.C. Iselin, CERN SL/90-13 (AP) Rev.4 (1995).
- [2] I. Ben-Zwi BNL, private communication (Dec 2003).
- [3] H. Braun et al., 20th Internat. Linac Conf. (2000) 98.
- [4] E. Keil, CERN-SL/2000-006 (AP) (2000).
- [5] K.Y. Ng in Handbook of Accelerator Physics and Engineering, A.W. Chao and M. Tigner, eds., 2nd printing (World Scientific, Singapore 2002) 94.
- [6] W. Schnell, *ibid.*, 526.
- [7] J.S. Berg and R.B. Palmer, Longitudinal Acceptance, FFAG Workshop, TRIUMF, April 2004.
- [8] E. Keil and A.M. Sessler, submitted to Nucl.Inst.Meth. A.